

Structure–Bioactivity Relationships of Lapatinib Derived Analogs against *Schistosoma mansoni*

Melissa J. Buskes, Monica Clements, Kelly A. Bachovchin, Hitesh B. Jalani, Allison Leonard, Seema Bag, Dana M. Klug, Baljinder Singh, Robert F. Campbell, Richard J. Sciotti, Nelly El-Sakkary, Conor R. Caffrey,* Michael P. Pollastri, and Lori Ferrins*

Cite This: *ACS Med. Chem. Lett.* 2020, 11, 258–265

Read Online

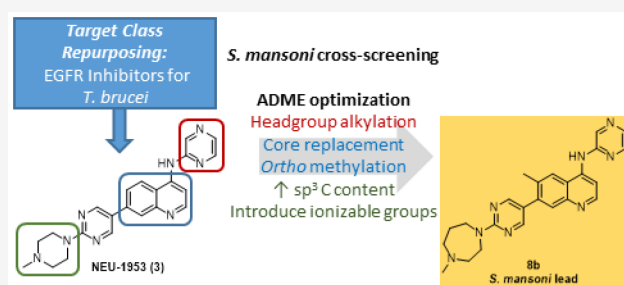
ACCESS |

Metrics & More

Article Recommendations

Supporting Information

ABSTRACT: We recently reported a series of compounds for a solubility-driven optimization campaign of antitrypanosomal compounds. Extending a parasite-hopping approach to the series, a subset of compounds from this library has been cross-screened for activity against the metazoan flatworm parasite, *Schistosoma mansoni*. This study reports the identification and preliminary development of several potentially bioactive compounds against adult schistosomes, one or more of which represent promising leads for further assessment and optimization.



KEYWORDS: Schistosomiasis, *Schistosoma* spp, Target class repurposing, Neglected tropical disease, Parasite-hopping

Schistosomiasis, caused by trematode flatworms of the genus *Schistosoma*, is a debilitating and serious parasitic neglected tropical disease (NTD) that leads to chronic ill-health.¹ There are two major forms of schistosomiasis infections, urogenital and intestinal. Urogenital schistosomiasis is caused by *S. hematobium*, and intestinal schistosomiasis is caused by *S. mansoni*, *S. japonicum*, *S. mekongi*, and *S. guineensis* (and related *S. intercalatum*).¹ The disease is currently treated and controlled with praziquantel; estimates show that at least 74 million people required treatment, and an additional 220 million people received prophylactic treatment in 2017.¹ Praziquantel is currently used against all *Schistosoma* species, but due to increasing concerns of resistance and inadequate efficacy there is a need for new therapeutics.² To shorten the timeline and costs associated with developing drugs against NTDs, repurposing efforts utilizing known drugs as starting points for chemical exploration and development can be employed.³

A target class repurposing approach was undertaken in order to optimize the U.S. Food and Drug Administration-approved drug lapatinib (Tykerb) (1) as an antitrypanosomal drug against *Trypanosoma brucei brucei* (Figure 1).⁴ A series of lapatinib-derived analogs were produced during medicinal chemistry optimization campaigns,^{5–8} ultimately resulting in the discovery of 3 (NEU-1953),⁸ a compound that displayed moderate antitrypanosomal potency.⁹ Subsequent efforts focused on the solubility-driven optimization of 3, while maintaining its antitrypanosomal potency and selectivity.¹⁰

Historically, we have cross-screened compounds arising from our different kinase inhibitor repurposing projects against

various parasites,^{5,9,11,12} and due to the known representation of protein kinases in *S. mansoni*,¹³ a subset of the compounds from this optimization campaign was screened against the parasite. Table 1 summarizes a set of desired properties for antischistosomal lead compounds that are based on a suggested target product profile for schistosomiasis^{2,14,15} and its emphasis on oral bioavailability. The *in vitro* ADME properties that are described were designed in-house with oral bioavailability in mind.

Because the schistosome parasite can present multiple and dynamic phenotypic responses to chemical insult,¹⁶ we employ a constrained nomenclature of descriptors to describe the changes in the parasite as a function of time and concentration (e.g., motility, density, and shape; and in the case of the adult parasite, an inability to adhere to the bottom of the assay dish). These descriptors are converted into severity scores on a scale of 0 (green)–4 (severest/red) that allow for partially quantitative comparisons of compound effects.^{17–20} Preference is given to those compounds that generate the highest severity score in the least time on the basis that highly active acute (single dose) therapies are part of the profile associated with a new drug to treat schistosomiasis.^{2,14,15} The descriptors themselves and their respective scores are detailed in the Supporting Information, Table S1. Severity score data are

Special Issue: Women in Medicinal Chemistry

Received: October 1, 2019

Accepted: January 10, 2020

Published: January 10, 2020

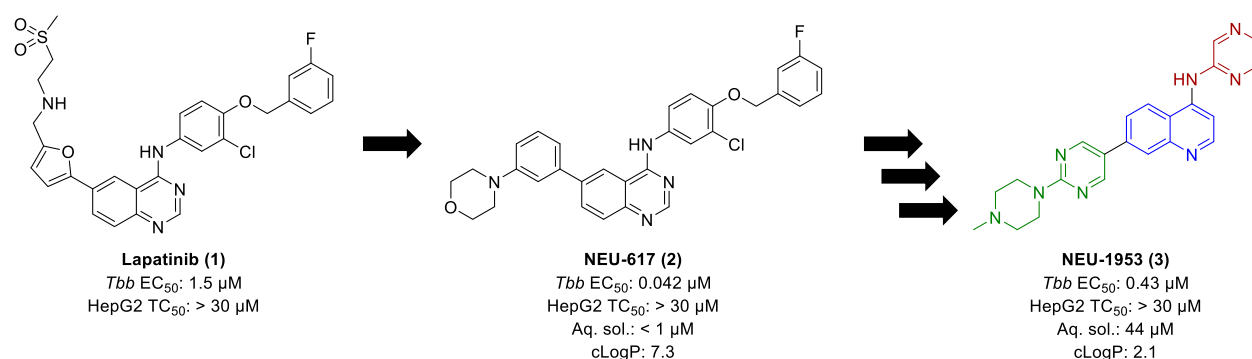


Figure 1. Target class repurposing of lapatinib as an antitrypanosomal compound.^{4–9} The different regions of exploration around 3 are denoted by color (head region is red; tail region is green; core is blue).

Table 1. Targeted *in Vitro* and *in Vivo* Properties for Antischistosomal Lead Compounds

	property	suggested minimum value or threshold
<i>in vitro</i> bioactivity and selectivity properties	<i>S. mansoni</i> severity score	at 10 μM ≥ 2 after 5 h or ≥ 3 after 24 h
	HepG2 TC ₅₀	≥ 5 μM after 48 h
<i>in vitro</i> ADME properties	human liver microsome clearance	Cl _{int} < 8.6 μL/min/mg protein
	rat hepatocyte clearance	Cl _{int} < 5.1 μL/min/10 ⁶ cells
	plasma protein binding (PPB)	< 95%
	thermodynamic solubility (pH = 7)	> 100 μM

presented in the results (with the corresponding descriptors detailed in the [Supporting Information, Tables S2–S8](#)), and

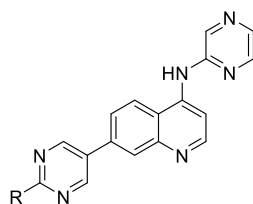
eight new analogs developed and synthesized in support of this effort are described. Finally, absorption, distribution, metabolism and excretion (ADME) data of all compounds presented in this work are reported in the [Supporting Information, Table S15](#).

When screened against adult *S. mansoni*, 3 displayed no bioactivity, which was also observed of the *tert*-butyl carbamate synthetic precursor 3a and a methylene carboxylic acid 3b ([Table 2](#)). Replacement of the piperazine with proline 3c maintains no bioactivity; however, its methyl ester derivative 3d displayed bioactivity after 24 h, progressing to the severest response by 48 h. This result may be due to the compound being a more cell-permeable pro-drug of 3c. Compound 3e, possessing a *tert*-butyl carbamate methylethylenediamine in place of the piperazine, displays a maximal phenotypic response after 48 h though this was also accompanied by an increase in toxicity versus HepG2 cells; however, both 3d and

Table 2. Phenotypic Changes, Expressed as Severity Scores, in *S. mansoni* and HepG2 TC₅₀ for Piperazine-Replacement Analogs 3a–3e

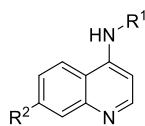
ID	R	Severity Scores (10 μM)				HepG2 TC ₅₀ (μM)
		1 h	5 h	24 h	48 h	
3 ^{8,9}		0	0	0	0	> 30
3a ¹⁰		0	0	0	0	> 30
3b ¹⁰		0	0	0	0	> 30
3c ¹⁰		0	0	0	0	> 30
3d ¹⁰		0	0	3	4	> 30
3e ¹⁰		0	0	0	4	8.0

Table 3. Phenotypic Changes, Expressed as Severity Scores, in *S. mansoni* and HepG2 TC₅₀ for Piperazine-Replacement, Increasing sp³ Carbon Content, Analogs 4a–4g

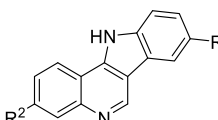


ID	R	Severity Scores (10 μM)				HepG2 TC ₅₀ (μM)
		1 h	5 h	24 h	48 h	
3 ^{8,9}		0	0	0	0	> 30
4a ¹⁰		0	0	1	1	37
4b ¹⁰		0	1	1	2	25
4c ¹⁰		0	1	2	4	36
4d ¹⁰		0	0	0	0	33
4e ¹⁰		0	0	0	0	> 36
4f ¹⁰		0	0	0	0	17
4g		0	0	0	0	25

Table 4. Phenotypic Changes, Expressed as Severity Scores, in *S. mansoni* and HepG2 TC₅₀ for 2-Aminopyrazine Headgroup Replacement Analogs 5a–5f



ID	R ¹	R ²	Severity Scores (10 μM)				HepG2 TC ₅₀ (μM)
			1 h	5 h	24 h	48 h	
3 ^{8,9}			0	0	0	0	> 30
5a			1	4	4	4	16
4d ¹⁰			0	0	0	0	33
5b ¹⁰			0	0	3	4	27
5c ¹¹			0	0	0	0	> 37
5d ¹¹			1	3	4	4	6.8
5e ¹¹			0	0	0	0	11
5f ¹¹			2	2	2	2	1.8

Table 5. Phenotypic Changes, Expressed as Severity Scores, in *S. mansoni* and HepG2 TC₅₀ for Isocryptolepine Analogs 6a–6c


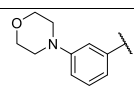
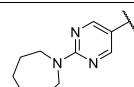

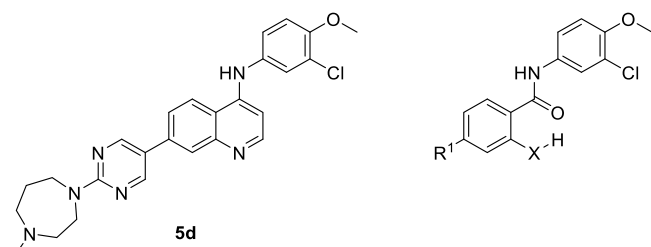
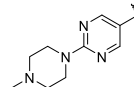
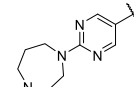
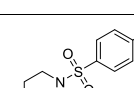
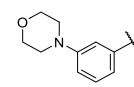
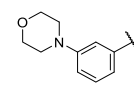
ID	R ¹	R ²	Severity Scores (10 μM)				HepG2 TC ₅₀ (μM)
			1 h	5 h	24 h	48 h	
6a ¹¹	-H		0	1	0	1	40
6b ¹¹	-H		0	1	1	4	7.4
6c ¹¹	-CH ₃		3	4	4	4	4.7

Table 6. Phenotypic Changes, Expressed as Severity Scores, in *S. mansoni* and HepG2 TC₅₀ for Pseudoring Analogs 7a–7e^a


ID	X	R ¹	Severity Scores (10 μM)				HepG2 TC ₅₀ (μM)
			1 h	5 h	24 h	48 h	
5d ¹¹			1	3	4	4	6.8
7a ¹⁰	-O-		0	0	0	nt	27
7b ¹⁰	-O-		0	1	2	4	> 6.5
7c ¹⁰	-O-		0	3	2	nt	> 29
7d ¹⁰	-O-		2	2	3	4	35
7e ¹⁰	-NH-		0	0	2	2	35

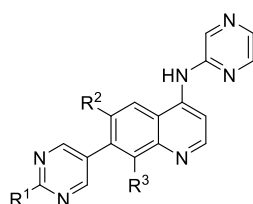
^ant = not tested.

3e display poor ADME profiles overall (see Supporting Information, Table S15).

Introduction of the bridged piperazine 4a improved aqueous solubility and metabolic stability in comparison to 3, though minimal bioactivity was observed after 48 h (Table 3). Extending the length of the piperazine alkyl chain to the ethyl (4b) and propyl (4c) resulted in activity after 5 h in both cases, with the propyl possessing the most severe phenotypic response after 48 h. Substitution of the piperazine for the N-

alkylhomopiperazine derivatives (4d–f), and the unsubstituted homopiperazine (4g) (synthesis detailed in Supporting Information, Scheme S1), improved the solubility of the compounds in comparison to 3. However, bioactivity of this series was not observed against adult schistosomes.

Replacing the 2-aminopyrazine headgroup of 3 with saturated rings (Supporting Information, Table S4) resulted in no significant bioactivity recorded for tertiary amines (S1a and S1b) or upon replacement of the 2-aminopyrazine with

Table 7. Phenotypic Changes, Expressed as Severity Scores, in *S. mansoni* and HepG2 TC₅₀ for *ortho*-Methylated Analogs 8a–8e and 9a–9e^a

ID	R ¹	R ²	R ³	Severity Scores (10 μM)				HepG2 TC ₅₀ (μM)
				1 h	5 h	24 h	48 h	
3 ^{8,9}		-H	-H	0	0	0	0	> 30
8a ¹⁰		-CH ₃	-H	2	3	4	4	5.9
8b		-CH ₃	-H	4	4	4	4	7.6
8c		-CH ₃	-H	0	4	4	4	4.7
8d		-CH ₃	-H	1	1	3	3	7.6
8e		-CH ₃	-H	0	0	0	0	13
9a ¹⁰		-H	-CH ₃	0	0	1	2	9.6
9b		-H	-CH ₃	0	0	0	0	nt
9c		-H	-CH ₃	0	0	0	0	16
9d		-H	-CH ₃	1	1	4	4	12
9e		-H	-CH ₃	0	2	4	4	> 3.7

^ant = not tested.

either a cyclohexanol (**S1c**), tetrahydropyran (**S1d**), or methylene tetrahydropyran (**S1e**). Overall, it was noted that while increasing the sp³ content of the headgroup did achieve improved aqueous solubility in comparison to **3**, these analogs displayed variable toxicity against HepG2 cells.

Notably, methylation at the 5-position of the 2-aminopyridine headgroup (**5a**) resulted in a severe phenotypic response after just 5 h, vastly different from the negligible bioactivity observed of **3** (Table 4). However, aqueous solubility and metabolic stability decreased, and toxicity against HepG2 cells increased greater than 1.9-fold. The *N*-methylhomopiperazine tail counterpart, **5b**, provided a potent compound with bioactivity recorded after 24 h, a later time point than **5a**. Although **5a** was a more potent antischistosomal lead, **5b** displayed a superior ADME profile. The unsubstituted 2-aminopyridine and pyrimidine headgroup analogs (**4d** and **5c**, respectively) led to a complete loss in activity, whereas

replacement with 3-chloro-4-methoxyphenyl (**5d**) (a truncated version of the lapatinib (**1**) headgroup) generated severe phenotypic responses, albeit it with a 7-fold decrease in aqueous solubility when compared to **3** and an undesirable ADME and selectivity profile. Replacement of the tail group of **5d** with a phenyl sulfonamide, *N*-methylhomopiperazine (**5e**), yielded a complete loss of bioactivity. However, maintaining this phenyl sulfonamide, *N*-methylhomopiperazine tail in the presence of a 3-chloropyridine headgroup (**5f**) resulted in moderate bioactivity recorded after 1 h, which remained consistent over time. In line with the structure–activity relationships (SAR) observed with respect to substitution on the headgroup (compounds **5a**, **5b**, **5d**), the presence of a substituent at the *para* position of the headgroup appears to increase potency of the compounds, and the presence of the nitrogen within the ring appears to be beneficial for potent activity. However, **5f** exhibited poor aqueous solubility and was

rapidly cleared in human liver microsomes (HLM) as well as being toxic to HepG2 cells (TC₅₀ 1.8 μM). Analogs were tested that investigated headgroup replacements, including saturated groups matched with various tails, although this time at the 6-position of the core (Supporting Information, Table S11). No notable activity against schistosomes was recorded, with the exception of compound **S3b** (pyrimidine headgroup in combination with a phenyl sulfonyl morpholine tail at the 6-position), which displayed moderate activity after 1 h.

Isocryptolepine analogs were tested (Table 5), initially possessing an unsubstituted headgroup (R¹ = H), and the tail group was modified from a phenylmorpholine of **6a** to the pyrimidine *N*-methylhomopiperazine of **6b**, which both showed minimal bioactivity after 5 h, with **6b** displaying potent activity after 48 h. Maintaining the pyrimidine *N*-methylhomopiperazine tail, methylation of the R¹ position (**6c**), resulted in severe bioactivity after 1 h. This result is in line with SAR trends observed previously where substitution on the headgroup appears to be beneficial to antischistosomal potency. However, **6c** displayed undesirable toxicity against HepG2 cells.

Pseudoring analogs matched to the bioactive **5d**, possessing the 2-chloro-4-methoxy headgroup and varying tail groups, are presented in Table 6. The direct pseudoring matched pair (**7b**) showed minimal bioactivity after 5 h and potent activity after 48 h. Replacement of the *N*-methylhomopiperazine to the *N*-methylpiperazine tail (**7a**) resulted in a complete loss of activity. Further, replacement of the tail with the phenyl-sulfonamide *N*-methylpiperazine (**7c**) produced a phenotypic response after 5 h. The *meta*-substituted phenylmorpholine (**7d**) displayed a phenotypic response after 1 h which increased in severity over time. Replacement of the –OH functionality of **7d** with the free amine yielded **7e**, a compound that was not as potent as its counterpart but displayed bioactivity after 24 h nonetheless. In general, this series displayed poor aqueous solubility. Additional pseudoring analogs were explored with alternate head and tail group variations; however, there was no notable activity reported (Supporting Information, Table S13).

Ortho-methylated core analogs were screened against *S. mansoni*, and the severity scores are presented in Table 7 with the ADME data of the series subsequently presented in Table 8. Installation of a methyl at the 6-position of the quinoline core (**8a**) resulted in a compound that showed a severe

phenotypic response by 5 h that subsequently increased over time. However, this compound also exhibited a greater than 5-fold increase in toxicity against HepG2 cells and a >2200-fold decrease in aqueous solubility compared with **3**. Alternatively, methylation at the 8-position of the quinoline (**9a**) provided a compound with moderate potency after 24 h; however, it exhibited poor physicochemical properties and toxicity against HepG2 cells. In an attempt to optimize the series, additional *ortho*-methylated analogs were designed to improve the antischistosomal activity and to exploit functionality that would improve the ADME and toxicity profile. We had already shown that replacement of the piperazine with a homopiperazine improved the ADME profile;¹⁰ as such, we substituted the piperazine for the homopiperazine and explored the effect of the length and presence of the alkyl chain.

A general synthetic scheme that closely follows one we previously reported¹⁰ for novel *ortho*-methylated analogs is presented in the Supporting Information (Scheme S2).

Focusing on the 6-methyl core, replacement of the piperazine with the *N*-methylhomopiperazine (**8b**) resulted in the most potent compound to date, with a severe phenotypic response recorded after 1 h. Extension of the alkyl chain to an ethyl (**8c**) provided a similar phenotypic response, further extension to a propyl (**8d**) resulted in bioactivity being detected after 1 h, and a more severe phenotypic response was recorded after 24 h. These compounds showed the greatest antischistosomal activity of the series, with **8b** possessing >33,500-fold improvement in solubility compared to **8a**; however, clearance increased 2-fold, and no toxicity improvement was observed. The unsubstituted homopiperazine (**8e**) improved metabolic stability 10-fold in comparison to **8a** and was modestly less toxic, though the compound was inactive against schistosomes.

The 8-methyl core was then explored. Although appreciably soluble, replacement of the *N*-methylpiperazine for the *N*-methylhomopiperazine (**9b**) and subsequent extension to the *N*-ethylhomopiperazine (**9c**) resulted in compounds that showed no bioactivity. Further extension of the alkyl chain improved potency, with the *N*-propylhomopiperazine (**9d**) strongly bioactive by 24 h. Unfortunately, this was accompanied by high HLM clearance and concerns with toxicity against HepG2 cells. Interestingly, the unsubstituted homopiperazine (**9e**) led to an analog with a phenotypic response after 5 h, which was not observed in its 6-methylated quinoline counterpart **8e**. Analog **9e** also exhibited improved metabolic stability.

A series of compounds designed to improve the physicochemical profile of an antitrypanosomal lead compound, NEU-1953 (**3**), were crossed-screened against adult *S. mansoni*. Four potent compounds of interest (**5a**, **5d**, **6c**, and **8a**) were identified, with the most promising possessing an *ortho*-methylated quinoline core. Compounds of this series were further explored, optimizing for antischistosomal activity, which resulted in **8b**—a promising lead—with **8a**, **8c**, and **9e** presenting as potential backup leads for further assessment and optimization as antischistosomal compounds.

■ ASSOCIATED CONTENT

Supporting Information

The Supporting Information is available free of charge at <https://pubs.acs.org/doi/10.1021/acsmchemlett.9b00455>.

Table 8. ADME Profile, Including Aqueous Solubility, Plasma Protein Binding, and Metabolic Stability, of *ortho*-Methylated Quinoline Analogs

ID	aq sol ^a (μM)	human PPB ^b (%)	HLM ^c Cl _{int} ^d (μL/min/mg protein)
3 ^{8,9}	44	87	180
8a ¹⁰	< 0.02	97	130
8b	670	82	260
8c	790	84	300
8d	480	88	300
8e	1000	70	13
9a ¹⁰	5.0	97	120
9b	860	82	120
9c	580	88	160
9d	450	94	300
9e	465	76	41

^aaq sol = aqueous solubility. ^bPPB = plasma protein binding. ^cHLM = human liver microsomes. ^dCl_{int} = intrinsic clearance.

Details of biological assay protocols, chemistry experimental, *in vitro* ADME properties, and additional supplementary data (PDF)

AUTHOR INFORMATION

Corresponding Authors

Conor R. Caffrey – University of California, San Diego, La Jolla, California; Email: ccaffrey@health.ucsd.edu

Lori Ferrins – Northeastern University, Boston, Massachusetts; orcid.org/0000-0001-8992-0919; Email: l.ferrins@northeastern.edu

Other Authors

Melissa J. Buskes – Northeastern University, Boston, Massachusetts; orcid.org/0000-0001-5673-9101

Monica Clements – Northeastern University, Boston, Massachusetts

Kelly A. Bachovchin – Northeastern University, Boston, Massachusetts

Hitesh B. Jalani – Northeastern University, Boston, Massachusetts; orcid.org/0000-0002-2442-9798

Allison Leonard – Northeastern University, Boston, Massachusetts

Seema Bag – Northeastern University, Boston, Massachusetts

Dana M. Klug – Northeastern University, Boston, Massachusetts

Baljinder Singh – Northeastern University, Boston, Massachusetts; orcid.org/0000-0003-2828-5768

Robert F. Campbell – Walter Reed Army Institute of Research, Silver Spring, Maryland

Richard J. Sciotti – Walter Reed Army Institute of Research, Silver Spring, Maryland

Nelly El-Sakkary – University of California, San Diego, La Jolla, California

Michael P. Pollastri – Northeastern University, Boston, Massachusetts; orcid.org/0000-0001-9943-7197

Complete contact information is available at:

<https://pubs.acs.org/10.1021/acsmchemlett.9b00455>

Notes

Material has been reviewed by the Walter Reed Army Institute of Research. There is no objection to its presentation and/or publication. The opinions or assertions contained herein are the private views of the author and are not to be construed as official or as reflecting true views of the Department of the Army or the Department of Defense.

The authors declare no competing financial interest.

ACKNOWLEDGMENTS

This work was supported by National Institutes of Health grants (R01AI082577, R56AI099476, R01AI124046, R21AI127594, R01AI126311, R01AI114685 to M.P.P.). M.C. acknowledges support for her internship at Northeastern from the National Research Foundation of South Africa. Phenotypic screens of *S. mansoni* were supported in part by R21AI126296 and OPP1171488 awards from the NIH-NIAID and Bill and Melinda Gates Foundation, respectively, to C.R.C. The *S. mansoni* life cycle was supported in part by snails and/or hamsters provided by the NIAID Schistosomiasis Resource

Center that were distributed through BEI Resources under the NIH-NIAID Contract HHSN272201700014I. A free academic license to OpenEye Scientific Software and ChemAxon for their suites of programs is gratefully acknowledged. We are grateful to AstraZeneca for the determination of *in vitro* ADME properties presented.

ABBREVIATIONS

S. mansoni, *Schistosoma mansoni*; NTD, neglected tropical disease; SAR, structure–activity relationships; HLM, human liver microsomes; Cl_{int} , intrinsic clearance; aq sol, aqueous solubility; PPB, plasma protein binding

REFERENCES

- (1) World Health Organization: Schistosomiasis. <https://www.who.int/schistosomiasis/en/>, (accessed Sept. 30, 2019).
- (2) Caffrey, C. R.; El-Sakkary, N.; Mäder, P.; Krieg, R.; Becker, K.; Schlitzer, M.; Drewry, D. H.; Vennerstrom, J. L.; Grevelding, C. G. In *Neglected Tropical Diseases: Drug Discovery and Development*; Swinney, D., Pollastri, M., Eds.; Wiley-VCH Verlag GmbH: Weinheim, Germany, 2019; pp 187–225, DOI: 10.1002/9783527808656.
- (3) Klug, D. M.; Gelb, M. H.; Pollastri, M. P. Repurposing strategies for tropical disease drug discovery. *Bioorg. Med. Chem. Lett.* **2016**, *26*, 2569–2576.
- (4) Patel, G.; Karver, C. E.; Behera, R.; Guyett, P. J.; Sullenberger, C.; Edwards, P.; Roncal, N. E.; Mensa-Wilmot, K.; Pollastri, M. P. Kinase Scaffold Repurposing for Neglected Disease Drug Discovery: Discovery of an Efficacious, Lapatatinib-Derived Lead Compound for Trypanosomiasis. *J. Med. Chem.* **2013**, *56*, 3820–3832.
- (5) Devine, W.; Woodring, J. L.; Swaminathan, U.; Amata, E.; Patel, G.; Erath, J.; Roncal, N. E.; Lee, P. J.; Leed, S. E.; Rodriguez, A.; Mensa-Wilmot, K.; Sciotti, R. J.; Pollastri, M. P. Protozoan parasite growth inhibitors discovered by cross-screening yield potent scaffolds for lead discovery. *J. Med. Chem.* **2015**, *58*, 5522–5537.
- (6) Devine, W.; Thomas, S. M.; Erath, J.; Bachovchin, K. A.; Lee, P. J.; Leed, S. E.; Rodriguez, A.; Sciotti, R. J.; Mensa-Wilmot, K.; Pollastri, M. P. Antiparasitic Lead Discovery: Toward Optimization of a Chemotype with Activity Against Multiple Protozoan Parasites. *ACS Med. Chem. Lett.* **2017**, *8*, 350–354.
- (7) Woodring, J. L.; Bachovchin, K. A.; Brady, K. G.; Gallerstein, M. F.; Erath, J.; Tanghe, S.; Leed, S. E.; Rodriguez, A.; Mensa-Wilmot, K.; Sciotti, R. J.; Pollastri, M. P. Optimization of physicochemical properties for 4-anilinoquinazoline inhibitors of trypanosome proliferation. *Eur. J. Med. Chem.* **2017**, *141*, 446–459.
- (8) Mehta, N.; Ferrins, L.; Leed, S. E.; Sciotti, R. J.; Pollastri, M. P. Optimization of Physicochemical Properties for 4-Anilinoquinoline Inhibitors of Plasmodium falciparum Proliferation. *ACS Infect. Dis.* **2018**, *4*, 577–591.
- (9) Ferrins, L.; Sharma, A.; Thomas, S. M.; Mehta, N.; Erath, J.; Tanghe, S.; Leed, S. E.; Rodriguez, A.; Mensa-Wilmot, K.; Sciotti, R. J.; Gillingwater, K.; Pollastri, M. P. Anilinoquinoline based inhibitors of trypanosomatid proliferation. *PLoS Neglected Trop. Dis.* **2018**, *12*, No. e0006834.
- (10) Bachovchin, K. A.; Sharma, A.; Bag, S.; Klug, D. M.; Schneider, K. M.; Singh, B.; Jalani, H. B.; Buskes, M. J.; Mehta, N.; Tanghe, S.; Momper, J. D.; Sciotti, R. J.; Rodriguez, A.; Mensa-Wilmot, K.; Pollastri, M. P.; Ferrins, L. Improvement of aqueous solubility of lapatinib-derived analogues: identification of a quinolinimine lead for human African trypanosomiasis drug development. *J. Med. Chem.* **2019**, *62*, 665–687.
- (11) Singh, B.; Bernatchez, J. A.; McCall, L.-I.; Calvet, C. M.; Eckermann, J.; Souza, J. M.; Thomas, D.; Silva, E. M.; Bachovchin, K. A.; Klug, D. M.; Jalani, H. B.; Bag, S.; Buskes, M. J.; Leed, S. E.; Roncal, N. E.; Penn, E. C.; Erath, J.; Rodriguez, A.; Sciotti, R. J.; Campbell, R. F.; McKerrow, J.; Siqueira-Neto, J. L.; Ferrins, L.; Pollastri, M. P. Scaffold and Parasite Hopping: Discovery of New

Protozoal Inhibitors. *ACS Med. Chem. Lett.* **2020**, DOI: 10.1021/acsmchemlett.9b00453.

(12) Klug, D. M.; Diaz-Gonzalez, R.; Perez-Moreno, G.; Ceballos-Perez, G.; Garcia-Hernandez, R.; Gomez-Perez, V.; Ruiz-Perez, L. M.; Rojas-Barros, D. I.; Gamarro, F.; Gonzalez-Pacanowska, D.; Martinez-Martinez, M. S.; Manzano, P.; Ferrins, L.; Caffrey, C. R.; Navarro, M.; Pollastri, M. P. Evaluation of a class of isatinoids identified from a high-throughput screen of human kinase inhibitors as anti-Sleeping Sickness agents. *PLoS Neglected Trop. Dis.* **2019**, *13*, No. e0007129.

(13) Walker, A. J.; Ressurreicao, M.; Rothermel, R. Exploring the function of protein kinases in schistosomes: perspectives from the laboratory and from comparative genomics. *Front. Genet.* **2014**, *5*, 229.

(14) Caffrey, C. R. Chemotherapy of schistosomiasis: present and future. *Curr. Opin. Chem. Biol.* **2007**, *11*, 433–439.

(15) Keiser, J.; Utzinger, J. Advances in the discovery and development of trematocidal drugs. *Expert Opin. Drug Discovery* **2007**, *2*, S9–S23.

(16) Abdulla, M.-H.; Ruelas, D. S.; Wolff, B.; Snedecor, J.; Lim, K.-C.; Xu, F.; Renslo, A. R.; Williams, J.; McKerrow, J. H.; Caffrey, C. R. Drug Discovery for Schistosomiasis: Hit and Lead Compounds Identified in a Library of Known Drugs by Medium-Throughput Phenotypic Screening. *PLoS Neglected Trop. Dis.* **2009**, *3*, No. e478.

(17) Probst, A.; Nguyen, T. N.; El-Sakkary, N.; Skinner, D.; Suzuki, B. M.; Buckner, F. S.; Gelb, M. H.; Caffrey, C. R.; Debnath, A. Bioactivity of Farnesyltransferase Inhibitors Against *Entamoeba histolytica* and *Schistosoma mansoni*. *Front. Cell. Infect. Microbiol.* **2019**, *9*, 180.

(18) Long, T.; Rojo-Arreola, L.; Shi, D.; El-Sakkary, N.; Jarnagin, K.; Rock, F.; Meewan, M.; Rascon, A. A.; Lin, L.; Cunningham, K. A.; Lemieux, G. A.; Podust, L.; Abagyan, R.; Ashrafi, K.; McKerrow, J. H.; Caffrey, C. R. Phenotypic, chemical and functional characterization of cyclic nucleotide phosphodiesterase 4 (PDE4) as a potential anthelmintic drug target. *PLoS Neglected Trop. Dis.* **2017**, *11*, No. e0005680.

(19) Long, T.; Neitz, R. J.; Beasley, R.; Kalyanaraman, C.; Suzuki, B. M.; Jacobson, M. P.; Dissous, C.; McKerrow, J. H.; Drewry, D. H.; Zuercher, W. J.; Singh, R.; Caffrey, C. R. Structure-bioactivity relationship for benzimidazole thiophene inhibitors of polo-like kinase 1 (PLK1), a potential drug target in *Schistosoma mansoni*. *PLoS Neglected Trop. Dis.* **2016**, *10*, No. e0004356.

(20) Kyere-Davies, G.; Agyare, C.; Boakye, Y. D.; Suzuki, B. M.; Caffrey, C. R. Effect of phenotypic screening of extracts and fractions of *Erythrophleum ivorense* leaf and stem bark on immature and adult stages of *Schistosoma mansoni*. *J. Parasitol. Res.* **2018**, *2018*, 9431467.